Improving the operational signal processing chain for faster acquisition of new objects to the French national catalogue of orbital objects

Manuel Pavy, Pascal Richard, Emmanuel Delande
CNES, DOA/SME/SE
Sébastien Théron
Magellium

ABSTRACT

The French Space Agency (*i.e. Centre National d'Etudes Spatiales*) (CNES) and the National Center of Scientific Research (*i.e. Centre National de Recherche Scientifique*) (CNRS) have been working on optical Space Surveillance and Tracking (SST) for many years using the fast telescope for transitory objects (*i.e. Télescope à Action Rapide pour les Objets Transitoires*) (TAROT). The CNES is also in charge to establish the spatial situation based on its French national catalogue of orbital objects[1]. This paper introduces how the operational catalogue system has been improved by acting on different levels and finally have been enhanced till to be able to acquire new objects in the national catalogue of orbital objects. The multidisciplinary aspect of the work is the key of the improvement: algorithm, network, computer science, image processing and astronomic skills have been mixed together to reach a new functionnality for the benefit of the Space Surveillance Awareness (SSA), including the following of artificial space objects.

1. INTRODUCTION

1.1 System components

Maintaining and updating the French national catalogue[1] of space objects involves several components. The subsystem dedicated to MEO, GEO, HEO[2] orbits is mainly composed of three elements:

1. The TAROT network [1] owned by the CNRS provides the brunt of the images of the GEO belt from three telescopes around the world:
   (a) Tarot Calern (TCA) in mainland France,
   (b) Tarot Chili (TCH) in Chile,
   (c) Tarot Réunion (TRE) in the Réunion island (France);
2. Image processing sofware for space objects detections (*i.e. TRaitement d'Image pour les détectiONs d'objets spatiaux*) (TRITON) extracts objects detected in each TAROT image, and provides their magnitude and angular coordinates from photometric and astrometric calibration [14];
3. The satellites observation, measurements and orbits for SST (*i.e. Observation des Satellites, Mesures et Orbites pour la Surveillance de l'Espace*) (OSMOSE) software suite maintains an up-to-date catalogue of space objects through:
   (a) the processing of the measurements produced by institutional and commercial partners as well as the in-house detections produced by TRITON software using TAROT observations [2],

[1]The catalogue consists in the knowledge of the orbital parameters of identified space objects
[2]MEO: Medium Earth Orbit; GEO: Geostationary Earth Orbit; HEO: Highly Elliptical Orbit

(b) the scheduling of the TAROT sensors for surveillance activities or targeted data acquisition [13] in collaboration with the European Union Space Surveillance and Tracking (EUSST)[3].

The national catalogue producer system forms an IT system which interacts with remote telescopes to control them, and to retrieve low-level products (L1) from them.[4]

1.2 System workflow

The architecture of the system is illutrated in fig. 1, and the workflow of the measurement production is depicted in fig. 2.

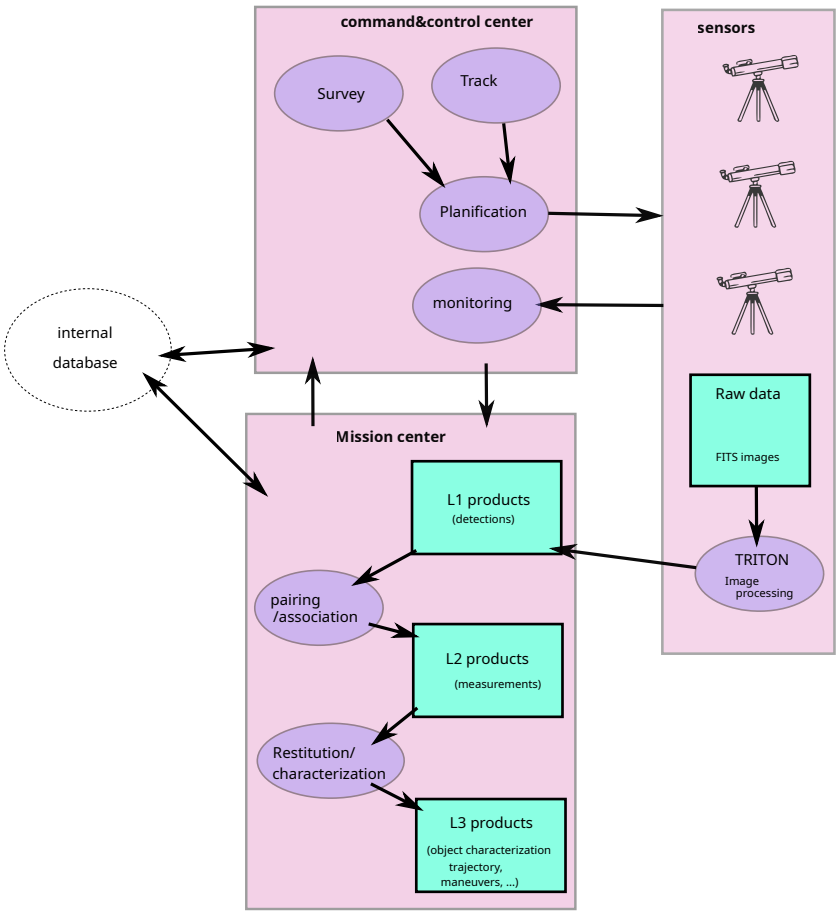

Fig. 1: IT system and life cycle of OSMOSE products from TAROT and TRITON

First, a TAROT telescope takes three successive photos, which are then processed by TRITON to extract the presence of objects in each image, called detections. Then, the OSMOSE software suite retrieves these detections, links them into tracklets (pairing step on fig. 2), and tries to associate this tracklet to objects already identified in the catalogue (association step on fig. 2).

The acquisition of new objects to the catalogue requires the ability to detect and track unknown objects by acquiring new measurements *in the same night*. It represents a real challenge: despite the daily update of about 500 catalogued objects, the full signal processing chain is a complex and time-consuming tasks.

Indeed, if the identification step (also called association step) fails, then OSMOSE must compute an initial orbit estimate from the orphan tracklet, then it is able to task the telescope network in order to observe the whereabouts of the potential object to confirm its existence through further observations.

[3]The EUSST is funded by the EU through the EU Space Programme and the Horizon Europe programmes

[4]The level product notion is inspired from the Earth Observing System Data and Information System (EOSDIS) [6].

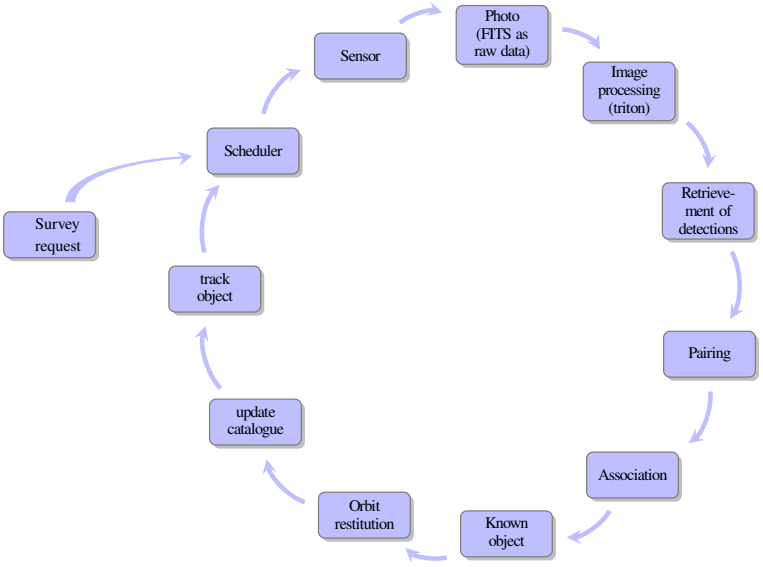

Fig. 2: Workflow of the OSMOSE survey and track processing chain

The first key improvement, covered in section 2 relates to the overhaul of the transmission protocol between the TAROT telescopes and the OSMOSE system. Owned by the CNRS and partially exploited by the CNES for SSA activities, these telescopes are located in remote areas and must rely on limited bandwidth for data transmission.

The second improvement, covered in section 3, relates to the processing of the TAROT images by the TRITON software, one of the most resource-intensive tasks within the processing chain. The principle of TRITON is to extract the brightest stars from the TAROT image, and link them to a star catalogue in order to a) compute the astrometric and photometric calibration of the picture and, then, b) extract objects from the image and provide angular pairs (right ascension and declination) for every such detection. This paper will present how an extract of GAIA[10] catalogue is built and used in production environment.

The last improvement, covered in section 4, deals with the overhaul of the orbit determination step, another major resource-intensive task in the processing of the OSMOSE software suite. It is only briefly covered in this paper, as it was the topic of recently published work [4]. The traditional approach, producing orbit estimates through least-square methods on 20-day-long observation arcs largely overlapping between two successive tracks, is replaced by a novel and quicker orbit restitution algorithm.

Finally, the paper will then show how these various improvements expanded the abilities of the OSMOSE cataloguing system to detect and incorporate new objects. Thanks to the improved reactivity of the overall processing chain, the OSMOSE software suite is then typically able to schedule further observations of a new object the same night it was detected, such that a confirmed object can be added to the catalogue sooner than before, more consistently, and with a higher quality orbit estimate.

2. OPTIMISATION OF COMMUNICATION WITH TELESCOPES

2.1 The importance of the downloaded volume

The TAROT network is deployed all around the Earth, from metropolitan France area to Chile and the Réunion island. In order to command and control these sensors on one hand and to retrieve the SSA information on the other hand, they are accessible through the Internet. As these remote areas are isolated, the OSMOSE and TAROT systems must be able to operate over an intermittent or low-speed Internet connection. One of the main principles to be rigorously applied is to limit the traffic to what it is strictly necessary. In that way, the images are processed on telescope site and only the image processing results (detections) are retrieved from the central system. The output is appended into a single file per day and this file is downloaded frequently in order to get fresh information and go on in the loop to track the object if necessary, as shown on fig. 2. Each image can provide several dozen lines; in this case, at the end

of the night, the file reached about 10 MB. For exemple, with a 100 kB s^{-1} bandwidth link, the download is done in 13 min 20 s, even if the useful data is less than 10 kB (the increased size from the previous download).

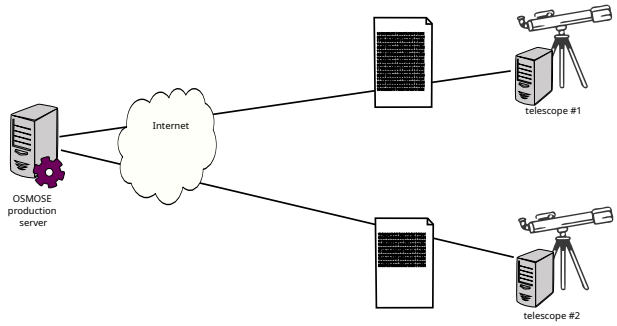

Fig. 3: Original data flow between telescope and OSMOSE server for production environment

2.2 Partial content

The HTTP protocol implement a feature to download partial content with code 206[9]:

```
HTTP/1.1 206 Partial Content
Date: Wed, 15 Nov 2015 06:25:24 GMT
Last-Modified: Wed, 15 Nov 2015 04:58:08 GMT
Content-Range: bytes 21010-47021/47022
Content-Length: 26012
Content-Type: image/gif
```

Code 1: Exemple of HTTP header for HTTP get on range request

In this example, the resource is 47,022 bytes long but the client requires only the end (from byte 21010 to byte 47021); consequently, the server send only 26012 (47021-21009) in the body response.

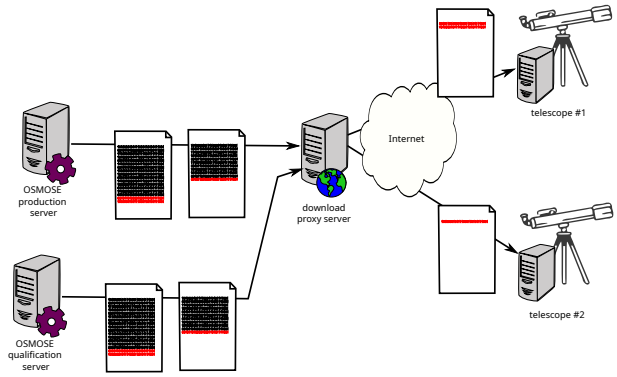

Fig. 4: Data flow between telescope and OSMOSE servers with the new solution.

Like almost all IT systems, OSMOSE is deployed on many environnements (dedicated to studies, integration or qualification in addition of the production one). To magnify the gain of the partial download, the architecture takes into account all these environments connected to the only server providing applicative proxy role as illustrated by fig. 4.

With that solution, the gain is that on each request the applicative proxy server serves different environments by avoiding loading the link with distant telescope server.

Table 1 shows how this simple change in method affects the downloads and can increase the reactivity of the chain.

Table 1: Comparison between the old methods (plain or gzip) and the new one. The best time is underlined for each case.

	File size	*Old method*		*Old method with Gzip*		*New method*	
		Data flow	*Time*	*Data flow*	*Time*	*Data flow*	*Time*
New file requested on a first environment	100 kB	100kB	8	25 kB	1 s	100 kB	8 s
New file requested on the second environment	100 kB	100kB	8 s	25 kB	1 s	200 B	1 s
10 kB appended data on 1 MB file	1 034 kB	1 034 kB	1min22	260 kB	2.5 s	10 kB	1 s
1 MB appended data on 5 MB file	6 MB	6 MB	8min	1.5 MB	2 min	1 MB	1min20
10 kB appended data on 10 MB file	10 MB	10 MB	13min20	2.5 MB	3min20	10 kB	1 s
1 MB appended data on 10 MB file	11 MB	11 MB	14min40	2.75 MB	3min40	1 MB	1min20
Total per night with 150kB per 10 min for 10 hours night	9 MB	275MB	Downloads KO after 8h20	69 MB		9 MB	
Total per night with 75kB per 5 min for 10 hours night	9 MB	545 MB	Downloads KO after 4h10	136 MB		9 MB	
For 2 environments	9 MB	1.1 GB		272 MB		9 MB	
Data recovery after unavailability of the network all the night long	9 MB	9 MB	12min	2.25 MB	3min	9 MB	12min

In case of data recovery due to network unavailability, the Gzip[5] method is still preferred.

2.3 Discarded approaches

Other promising approaches were explored, but ultimately discared as they incurred significant drawbacks or constraints:

- Usage of one result file per processed image:
  - One needs to request many files and manage the new file availability,
  - One needs to change the software on telescopes,
  - In case of failure, the diagnostic is more complicated due to the poor quality of the network link;
- Usage of web sockets[8]:
  - This technology is quite recent and not so proven as the existing one,
  - One needs to develop a functionality to manage disconnection/reconnection,

In the context of operational systems, availability, straightforwardness and reliability is overriding and the applicative proxy with range request solution was chosen for these reasons. The impact is that the system has reduced its data transfer consumption by 120 (or by 30 compared to the gzip evolution method) and is not impacted by increasing the refresh frequency.

3. OPTIMISATION OF ASTROMETRIC REDUCTION

The goal of astrometric reduction is to produce detections from visual images from the direction of the objects in celestial coordinates, and determine the magnitude and the size of the streaks. Following the calibration, information

related to stars in the images is filtered out, and detections provide the object coordinates at the time of the photo based on the positions of the stars.

The pointing and motorization information is used to:

1. Select the part of celestial sphere to be extracted from the star catalogue,
2. Compute the shape of the streaks to be identified as stars.

The astrometric calibration is illustrated in fig. 5, where segments between the predicted and the observed position of some of the stars detected in the image are used to establish the calibration function which computes the celestial direction of space objects given their coordinates in the picture.

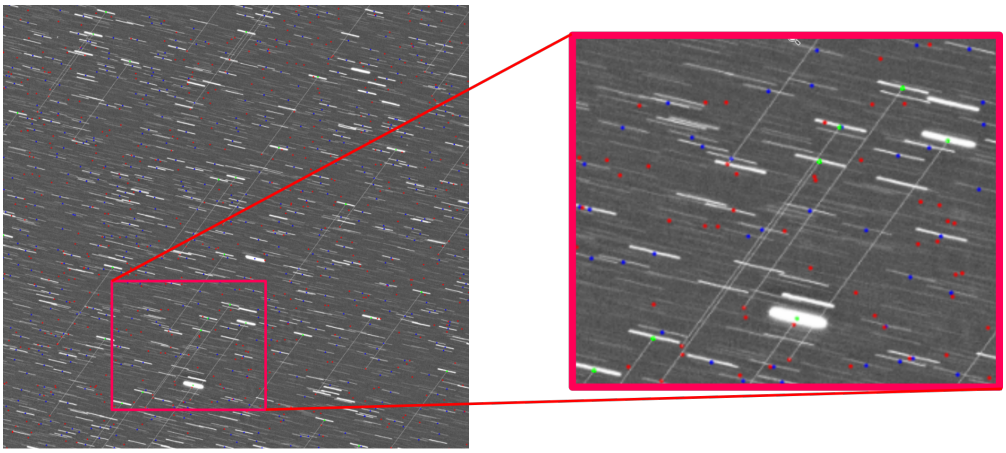

Fig. 5: Principle of astrometric calibration. Red dots correspond to the predicted stars positions based on the catalogue, blue dots are the detected stars in the image, and green dots are the stars considered to compute the calibration.

3.1 A Gaïa sub-catalogue selected for TRITON/TAROT space surveillance needs

Historically, the catalogue using by TRITON for astrometric reduction was the fourth U.S. Naval Observatory CCD Astrograph Catalog (UCAC4) [15]. This catalogue is simple and provides solid results. Nevertheless, in order to be even more precise, the latest releases of TRITON are able to use GAIA DR2 restricted to astrometry and photometry for non-professionals (*i.e. GAIA DR2 Restreint à l'Astrométrie et à la Photométrie Pour les Amateurs*) (GRAPPA2)[5] and take into account the proper motion effect of stars.

Thanks to the GAIA catalogue[3], GRAPPA2 is more accurate and allows for a better prediction of the positions of the stars in the image.

The TRITON astrometric calibration algorithm is based on the Groth triangles pairing method [11]. Due to exponential combinatorics leading to significant computational costs, the implementation of this method is limited here to 50 detected stars, or 55 stars from the star catalogue, inside an image tile (4 tiles per image). GRAPPA2 is very heavy and much information are not be used by our processing chain. Indeed, it provides 1,692,919,135 light sources information and store the data in 1,013,770 files within tree structure and takes 70 GB on disk.

In consequence, a new file based on GRAPPA2 format was built by limiting the number of stars per field of view, as well as the number of fields from the original catalogue; the result is a unique 170 MB file - see table 2.

Because,

1. an healpix level 6 tile has a $0.83^\circ \times 0.83^\circ$ field of view per tile [12],
2. the TAROT telescopes have fields of view with sizes ranging from $1.86^\circ \times 1.86^\circ$ or $4.2^\circ \times 4.2^\circ$,

[5] Based on GAIA DR2, the format of this catalogue was produced by Marc SERRAU from the Institute of Celestial Mechanics and Ephemeris Calculations (*i.e. Institut de Mécanique Céleste et de Calculs des Ephémérides*) (IMCCE) at the CNRS.

3. tiles from healpix and from telescope cannot overlap,
4. the first result with 30 stars per healpix level 6 tile catalogue are correct

Thus,

1. even if a part of the sky has fewer stars, the catalogue do not provide less star per image,
2. the smallest tiles of images have a $0.93° \times 0.93°$ field of view
3. for operation needs, the catalogue is built with one hundred stars per healpix level 6 tile.

3.2 Construction of the sub-catalogue

From the esac website[6], it is possible to retrieve stars from catalogue filtered by healpix function result (see Code 2).

```
curl -i -X POST --data "PHASE=run\&LANG=ADQL\&LANG=ADQL\&REQUEST=doQuery\&QUERY=SELECT+TOP
↪ +100+gaia_healpix_index(6,+source_id)+AS+healpix6,+source_id,+ra,+dec,+pmra,pmdec,+
↪ phot_g_mean_mag,+phot_bp_mean_mag,+phot_rp_mean_mag+FROM+gaiaedr3.gaia_source+WHERE+
↪ gaia_healpix_index(6,+source_id)+=+12=run\&LANG=ADQY+phot_g_mean_mag\&format=csv" "https://
↪ gea.esac.esa.int/tap-server/tap/async"
```

Code 2: Example of curl command to get the 100 brightest stars in the healpix level 6 tile 12.

This query provides the URL where the result will be available; for instance:

```
Location: https://gea.esac.esa.int/tap-server/tap/async/16879532231610
```

Code 3: Example of return command with the URL of the order.

The next step is to wait for a while, then download the product when available:

```
curl https://gea.esac.esa.int/tap-server/tap/async/16879532231610/results/result -o tile-12.
↪ res
```

Code 4: curl command to retrieve the result of the previously order.

```
head -4 tile-12.res
healpix6,source_id,ra,dec,pmra,pmdec,phot_g_mean_mag,phot_bp_mean_mag,phot_rp_mean_mag
12,1753553543188992,45.46359917458231,3.138095461386887,1.82787636211724,
↪ 9.885086354334051,8.163041,8.197672,8.071199
12,1743000808216320,45.10456694653876,2.9042785609486246,29.89899715192888,
↪ 94.09646041222076,9.690047,9.988975,9.223375
12,1791761572209792,44.55738022314381,3.1689625950941394,-19.478022694971642,
↪ -65.71716972703896,9.767177,10.074922,9.293641
```

Code 5: insight of the result file.

In order to get the full catalogue, this same query has to be executed for each tile (from 0 to 49,151) and the results are concatenated into a single file long of 1,474,561 lines. Then, this custom catalogue can be encoded as binary file.

3.3 Results and comparison

As fig. 6 shows, although the custom catalogue[7] extracts less stars per image (fig. 6a), this does not affect the quality of the astrometric calibration (fig. 6b).

[6] https://archives.esac.esa.int, i.e., the website from the European Space Agency (ESA) dedicated to the distributition GAIA products.

[7] The result concerning the custom catalogue is based on a catalogue referencing 30 stars per healpix tile, the operationnal chain is based on a catalogue referencing 100 stars which must be, consequently, more accurate

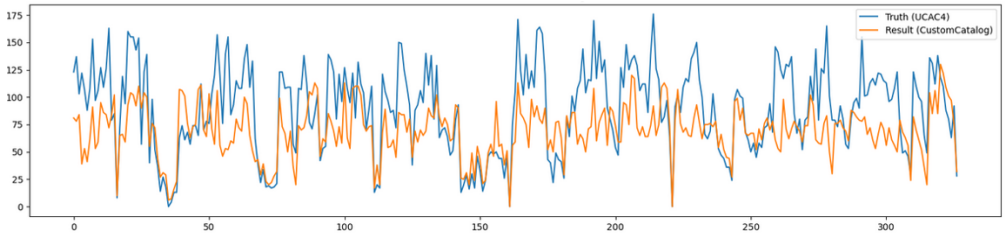

(a) Number of stars used

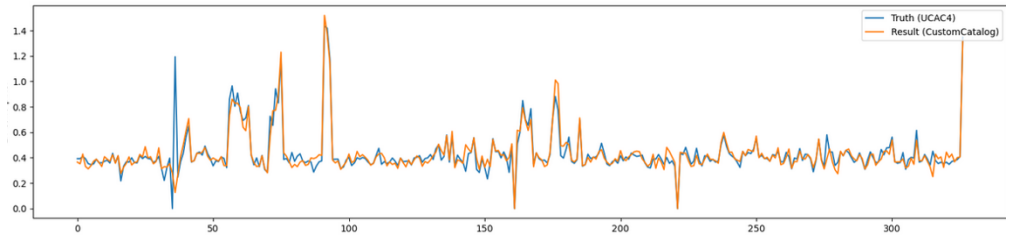

(b) Astrometric calibration error (in pixel)

Fig. 6: Astrometric calibration in TRITON as a function of image number for the old method (blue plot) and for the new one (orange plot)

Table 2: comparison of the star catalogue characteristics

	UCAC4 (ref)	*GRAPPA 2*	*Custom*
Number of stars	113,780,093	1,692,919,135	4,915,200
Accuracy at mag. 14	20 mas[15]	16 µas[7]	16 µas
Size of the catalogue	8.6 GB	70 GB	170 MB
Number of files	904	1,013,770	1
IO ratio in triton use vs ref	1	+57%	-22%
Magnitude of the faintest star	16	20	13.65

Basically, as shown in table 2, astrometric calibration with the custom catalogue needs two time less input/output storage on disk. In addition, considering the size of data file, the custom catalogue can be available permanently in Random Access Memory (RAM) and, in a repetitive contexct, TRITON do not have to physically read disk for getting catalogue data.

In addition, deploying the catalogue requires the sending of 170 MB to the telescope, taking – with a bandwidth of 200 kB s^{-1} – 2 h 35 min. In comparison, sending the full GRAPPA2 catalogue (70 GB) would take 32 days.

Finally, to cross-validate the evolution, the comparison has been done by processing the residuals of measurements against the precise object ephemeride, for the historical catalogue and for the new one[7]. The process have been done from the same images and have been plotted on fig. 7: it describes the residuals of the right ascension angle (fig. 7a) and of the declination angle (fig. 7b) as a function of time given as day number. The summary (table 3) confirms that the new method enhance the final measurement quality with a light reduction of the residuals on each variable.

Table 3: Summary of the comparison of measurement residuals with the old method vs the new one

	Old method	*New method*
Mean RAcos(DEC)	-1.765e-04 deg	-1.692e-04 deg
Standard deviation RAcos(DEC)	1.403e-04 deg	1.183e-04 deg
Mean RA_ICRS	-2.233e-04 deg	-2.105e-04 deg
Standard deviation RA_ICRS	-2.233e-04 deg	1.514e-04 deg
Mean DEC_ICRS	6.582e-05 deg	1.566e-05 deg
Standard deviation DEC_ICRS	1.860e-04 deg	1.757e-04 deg

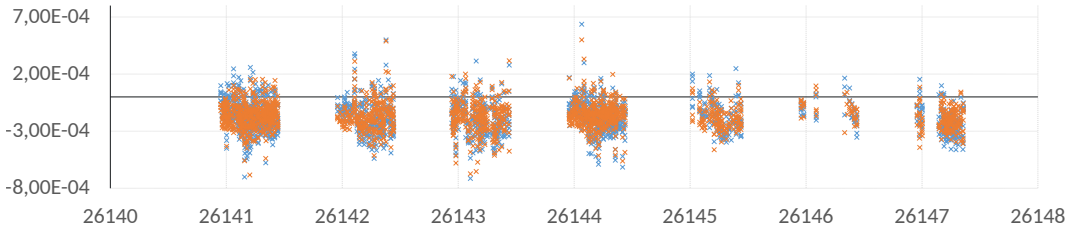

(a) Residuals on right ascension angle (in degree)

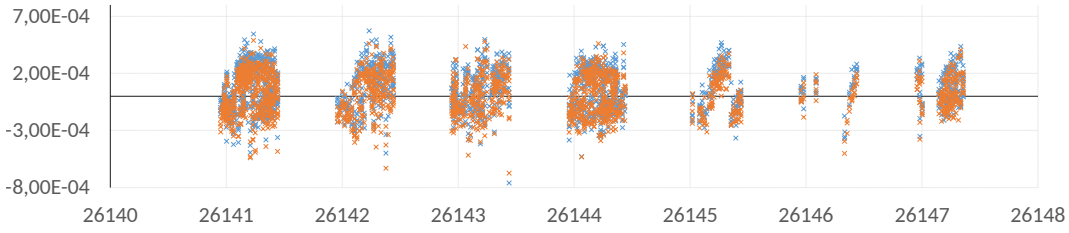

(b) Residuals on declination angle (in degree)

Fig. 7: Comparison of measurement residuals with the old method (in blue) vs the new one (in orange) as a function of day number

4. ORBIT RESTITUTION

Among the whole signal processing chain of the OSMOSE software suite, orbit determination is one of the most computationally intensive step.

OSMOSE exploits a least-square approach to generate new tracks. The former method did not consider the covariance of the input track, and relied instead upon 20-day-long observation arcs to generate new tracks, such that two successive tracks were based on largely overlapping arcs. In consequence the orbit determination step was time-consuming, especially while handling maneuvers, and the covariance of output tracks could not be easily exploited further (e.g. for the data association step).

A new orbit determination method has been recently developed for the OSMOSE software suite [4], summarized briefly here for the sake of completeness. While the new method is still based on a least-square approach, it aims to exploit the covariance of the input track *and* to consider only the measurements generated since the input track as observation arc. In that manner a) the orbit determination works on a much faster pace, and b) the covariance of each track represents the total information aggregated on the corresponding object up to that date, and is exploitable as such in other applications of the OSMOSE suite – most importantly, it can drive the data association step. Specific provisions have been to handle potential maneuvers detected during the orbit restiution step, namely:

1. *Short* tracks are produced on a fast pace (every three hours or so), based only on the few measurements (if any) generated since the latest available track in the database. If the orbit determination step fails, then it is re-attempted with an additive covariance term on the input track, accouting for the modeling mismatch induced by the potential maneuver. Several covariance terms are tried successively, sweeping a range of maneuvering profiles (in plane maneuvers, out of plane maneuvers, combined maneuvers, ...) of various magnitude. If the orbit determination step succeeds with a given covariance term, then the track is marked as *maneuvering*' in the OSMOSE database. Short tracks are the forefront of the dataflow, they are highly reactive to potential maneuvers but provide jittery estimates, especially during periods where maneuvers are frequent;

2. *Reference* tracks are produced on a longer pace (every day or so), based on all the measurements since either the earliest reference track in the last 20 days or the latest maneuvering track, whichever is the most recent. Reference tracks are thus built on observation arcs void of maneuvers – at least, void of those detected by the short tracks – and provide much smoother orbit estimates that the short tracks.

Overall, the new orbit determination method is computationally faster, much more reactive to maneuvers, and provides

an enriched orbit estimate through the covariance tracks [4]. It also avoid consuming computing power to re-propagate the trajectory on overlapping arcs. Moreover, it has the ability to reduce the time to first orbit determination after manoeuvers of the objects.

To be complete, taking into account physical constraints and experience, the system is equipped with covariance profiles corresponding to classical maneuvers (in plane maneuvers, out of plane maneuvers, combined maneuvers, ...) which are successively tried.

5. CONSEQUENCE OF THE REACTIVITY IMPROVEMENT

Thanks to all these improvements, the OSMOSE system is now able to react in about 75 minutes after the acquisition of a serie of images where an unknown object appears: it also can plan another observation to confirm or adapt the trajectory of the object, then reference it as a new object in the national catalogue if applicable.

If the data association step cannot find a suitable candidate for a newly produced tracklet , a re-observation loop triggers in order to determine an initial orbit and to attempt to track the object (see fig. 8). Once the re-observation loop has been completed the necessary number of times for the orbit determination step to converge, the system proposes a new object to be referenced in the catalogue. The operator can authorize the creation of the object in the catalogue, or let the system acquire more measurements before re-attempting the orbit determination process.

Table 4 shows some examples of the re-observation process, in which the system acquire in autonomous way new measurements by pointing unknown objects.

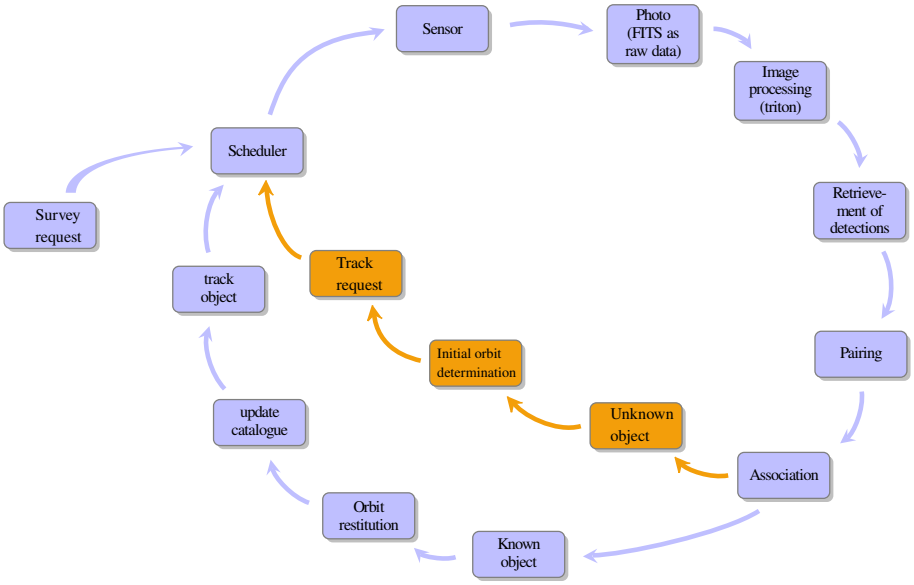

Fig. 8: Workflow of the OSMOSE surveillance and tracking processing chain. The short loop (re-observation process) is highlighted in orange.

Table 4: Examples of re-observation process chronogram

Day of the triggered re-observation	*Last image of a scene with unknown object*	*New pointing request*	*Re-observation pointing start*	*New measurement*
2023-01-08	04:20:59	04:36:06	05:35:01	05:35:28
2023-02-03	08:04:17	08:16:31	09:15:01	09:15:26
2023-02-04	23:43:27	23:56:33	01:00:13	01:00:37
2023-07-14	00:54:25	01:05:27	02:05:01	02:05:26
2023-07-21	00:56:16	01:10:31	02:13:40	02:14:05
2023-07-23	01:23:30	01:35:31	02:35:39	02:36:04

6. ACKNOWLEDGEMENT

This work has made use of data from the European Space Agency (ESA) mission Gaia (https://www.cosmos.esa.int/gaia), processed by the Gaia Data Processing and Analysis Consortium (DPAC, https://www.cosmos.esa.int/web/gaia/dpac/consortium). Funding for the DPAC has been provided by national institutions, in particular the institutions participating in the Gaia Multilateral Agreement.

The TAROT programme is funded by the CNRS.

The authors would like to thank the European Union, as both the TAROT and OSMOSE projects are partially funded by the EUSST programme. Warm thanks are also due to the crews of the observatories at le Calern, les Makes and la Silla for their help in shaping TAROT into a reliable and potent tool.

7. REFERENCES

[1] M. Boer, C. Thiebaut, A. Klotz, G. Buchholtz, A. L. Melchior, C. Pennypacker, and T. Ebisuzaki. Hands-on tarot: Intercontinental use of the tarot for education and public outreach, 2001.

[2] Michel Boër, Alain Klotz, Romain Laugier, Pascal Richard, Juan Carlos Dolado Pérez, Laurent Lapasset, Agnès Verzeni, Sébastien Théron, David Coward, and J.A. Kennewell. TAROT: a network for space surveillance and tracking operations. In *7th European Conference on Space Debris ESA/ESOC, Darmstadt/Germany*, Darmstadt, Germany, April 2017. ESA.

[3] Gaia Collaboration et al. Description of the gaia mission (spacecraft, instruments, survey and measurement principles, and operations). *Gaia Collaboration et al.(2016a): Summary description of Gaia DR1*, 2016.

[4] E. Delande, F. Thuillet, P. Richard, V. Baral, and M. Pavy. A novel, fast-paced orbit determination method for the cnes catalogue. In *Space traffic management conference*, Austin, 2023.

[5] Peter Deutsch. Gzip file format specification version 4.3. Technical report, 1996.

[6] Liping Di and Ben Kobler. Nasa standards for earth remote sensing data. *International Archives of Photogrammetry and Remote Sensing*, 33(B2; PART 2):147–155, 2000.

[7] ESA. Gaia Mission Science Performance - Gaia - Cosmos — cosmos.esa.int. https://www.cosmos.esa.int/web/gaia/science-performance. [Accessed 18-08-2023].

[8] Ian Fette and Alexey Melnikov. The websocket protocol. Technical report, 2011.

[9] R. Fielding, J. Gettys, J. Mogul, H. Frystyk, and T. Berners-Lee. Rfc2068: Hypertext transfer protocol – http/1.1, 1997.

[10] Gaia Collaboration, Brown, A. G. A., Vallenari, A., Prusti, T., de Bruijne, J. H. J., and al. Gaia early data release 3 - summary of the contents and survey properties. *A&A*, 649:A1, 2021.

[11] Edward J Groth. A pattern-matching algorithm for two-dimensional coordinate lists. *Astronomical Journal (ISSN 0004-6256), vol. 91, May 1986, p. 1244-1248.*, 91:1244–1248, 1986.

[12] K. M. Górski, E. Hivon, A. J. Banday, B. D. Wandelt, F. K. Hansen, M. Reinecke, and M. Bartelmann. Healpix: A framework for high-resolution discretization and fast analysis of data distributed on the sphere. *The Astrophysical Journal*, 622(2):759, apr 2005.

[13] Vincent Morand, J Alves, J Gelhaus, S George, J Hermoso, and E Vellutini. System level studies to design optical surveillance networks in the frame of the eusst support framework. In *Proceedings of Advanced Maui Optical and Space Surveillance Technologies Cenference (AMOS), Conference*, 2018.

[14] C. Thiebaut, S. Theron, P. Richard, G. Blanchet, A. Klotz, and M. Boër. Image processing improvement for optical observations of space debris with the TAROT telescopes. In Gianluca Chiozzi and Juan C. Guzman, editors, *Software and Cyberinfrastructure for Astronomy IV*, volume 9913, page 99134G. International Society for Optics and Photonics, SPIE, 2016.

[15] N. Zacharias, C. T. Finch, T. M. Girard, A. Henden, J. L. Bartlett, D. G. Monet, and M. I. Zacharias. The fourth us naval observatory ccd astrograph catalog (ucac4). *The Astronomical Journal*, 145(2):44, jan 2013.